

Experimental determination of the ratio of the cross sections for ionization by protons of L_1 and L_2 atomic subshells

V. P. Petukhov, V. S. Nikolaev, E. A. Romanovskii, and V. A. Sergeev

Nuclear Physics Institute of the Moscow State University
(Submitted March 15, 1976)
Zh. Eksp. Teor. Fiz. 71, 968-974 (September 1976)

The results of an experimental determination of the ratio of the cross sections for ionization of the L_1 and L_2 subshells of palladium, antimony, and lanthanum atoms by 250-500-keV protons are presented. The cross-section ratios were determined from the proton-energy dependences of the characteristic x-ray intensities. The experimental results agree with Born-approximation calculations using Coulomb wave functions for the electrons and indicate that the ionization cross section depends strongly on features of the initial-state electron-momentum distribution.

PACS numbers: 34.50.Hc

Born-approximation calculations of the ionization cross sections of hydrogenlike ions and atoms in $2s$ and $2p$ states have shown^[1] that the ratio of these cross sections (σ_{2s} and σ_{2p}) is strongly dependent on the relative velocity v of the colliding particles whenever that velocity is smaller than the mean orbital velocity $v_0 Z/2$ of the removed electron ($v_0 = e^2/\hbar = 2.19 \cdot 10^8$ cm/sec and Z is the nuclear charge). This dependence of σ_{2p}/σ_{2s} is due to a corresponding behavior of the momentum distribution ratio $|\Phi_{2p}(p)|^2/|\Phi_{2s}(p)|^2$ for the electrons in these states and should therefore also be observed in the ionization of L_1 and L_2 atomic subshells^[2]; the latter has been treated theoretically^[3,4] using Coulomb wave functions for the electrons.

To test this conclusion we undertook an experimental determination of the cross-section ratio for ionization by protons of the L_1 and L_2 subshells of atoms for which the L -electron binding energy I is close to 4 keV. The results of these measurements, together with the recently published results of similar measurements for atoms with $I = 11-16$ keV,^[5-7] are compared with Born-approximation calculations.

1. EXPERIMENTAL TECHNIQUE

Removing $2s$ and $2p$ electrons from the L_1 and L_2 atomic subshells, respectively, leads to the emission of a series of characteristic lines, including the $L_{\beta 1}$ and $L_{\beta 3}$ lines (see the level diagram in Fig. 2), and from measurements of the intensities of these lines one can determine the ionization cross sections of the L_1 and L_2 subshells. In the case of thick targets, i. e., when the target thickness exceeds the range of protons of energy E in the target material, the relation between the cross section $\sigma_{\beta i}(E)$ for producing radiation in the line $L_{\beta i}$ and the intensity $J_{\beta i}(E)$ of the x radiation in this line is given by the formula^[3]

$$\sigma_{\beta i} = \frac{1}{n} \left[\frac{dJ_{\beta i}(E)}{dE} S(E) + \bar{\mu}_{\beta i} J_{\beta i}(E) \right], \quad (1)$$

where $S(E)$ is the proton stopping power of the target material, $\bar{\mu}_{\beta i}$ is the mass absorption coefficient of the target material for the corresponding line, and n is the

atomic density of the target.

The quantities $\sigma_{\beta 3}$ and $\sigma_{\beta 1}$ are related to the cross sections σ_{L_1} and σ_{L_2} for ionization of the L_1 and L_2 subshells by the formulas

$$\sigma_{\beta 3} = \sigma_{L_1} \omega_1 \Gamma_{\beta 3} / \Gamma_1, \quad \sigma_{\beta 1} = (\sigma_{L_2} + f_{12} \sigma_{L_1}) \omega_2 \Gamma_{\beta 1} / \Gamma_2, \quad (2)$$

in which $\Gamma_{\beta 1}$, $\Gamma_{\beta 3}$, Γ_1 , and Γ_2 are the partial and total radiative widths, ω_1 and ω_2 are the fluorescence yields corresponding to filling of the vacancies in the L_1 and L_2 subshells, and f_{12} is the Coster-Kronig factor.

From Eqs. (1) and (2) we obtain the following expression for the cross-section ratio:

$$\frac{\sigma_{L_2}}{\sigma_{L_1}} = \frac{\omega_1 \Gamma_{\beta 3} \Gamma_2}{\omega_2 \Gamma_1 \Gamma_{\beta 1}} \frac{(dJ_{\beta 1}/dE)S(E) + \bar{\mu}_{\beta 1} J_{\beta 1}}{(dJ_{\beta 3}/dE)S(E) + \bar{\mu}_{\beta 3} J_{\beta 3}} - f_{12}. \quad (3)$$

Thus, knowing the values of ω_1/ω_2 , $\Gamma_{\beta 3}/\Gamma_1$, $\Gamma_{\beta 1}/\Gamma_2$, $\bar{\mu}_{\beta 1}$, and f_{12} , we can determine the ratio $\sigma_{L_2}/\sigma_{L_1}$ of the L_2 - and L_1 -subshell ionization cross sections from measurements of the intensities of the $L_{\beta 1}$ and $L_{\beta 3}$ lines at various incident-proton energies E .

In our experimental setup (Fig. 1) a 4-mm diameter proton beam struck the target at an angle of 45° . The x radiation excited in the target passed through a Soller collimator set at 90° to the proton beam and, after reflection from the analyzing crystal, was registered with a proportional counter. The counter pulses were amplified in a linear amplifier and were fed to a differential discriminator, whose output was brought to a scaling circuit. In our experiments we used single crystals of lithium fluoride ($2d = 4.02$) and quartz ($2d = 6.66 \text{ \AA}$) as analyzing crystals. The analyzing crystal could be turned by a stepping motor to angles ranging from 15 to 60° .

In recording an x-ray spectrum, the counter pulses were registered during the accumulation of a specified charge by the beam-current integrator. Then a signal was sent to the stepping-motor control unit, which caused the crystal to be turned through a specified angle ($4'-8'$). The angular position of the crystal was monitored by a type F-5007 reversing counter, which kept track of the number of working pulses received by the

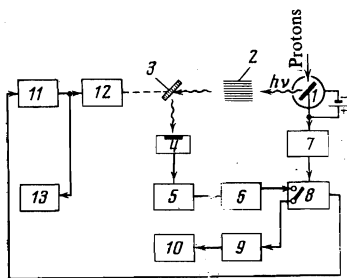


FIG. 1. Experimental setup: 1—target, 2—collimator, 3—analyzing crystal, 4—counter, 5—preamplifier, 6—amplifier, 7—current integrator, 8—scaler, 9—discriminator, 10—scaler, 11—stepping motor control unit, 12—stepping motor, 13—reversing counter.

stepping motor. Then the system for recording the x-ray photons and beam current was again put into operation and the entire cycle was repeated. As an example, in Fig. 2 we show a portion of the x-ray spectrum in the vicinity of the L_{β_1} and L_{β_3} lines, which was obtained by bombarding an antimony target with 450-keV protons. The photon-energy difference between the two lines is 90 eV, while the spectrometer resolution is 30 eV.

Since the energies of the x-ray quanta corresponding to the L_{β_1} and L_{β_3} lines differ by not more than 3%, the slight difference in recording efficiency for the two lines can be neglected and the quantities J_{β_i} and dJ_{β_i}/dE in Eq. (3) can be replaced by N_{β_i} and dN_{β_i}/dE , where N_{β_i} is the number of counts corresponding to L_{β_i} radiation during passage of a definite number of protons through the target. N_{β_i} was determined from the area under the L_{β_i} peak after subtracting the background.

To determine the ionization cross sections we measured the x-ray intensity as a function of the incident-particle energy. In our experiments the targets were palladium, antimony, and lanthanum foils 0.1–0.5 mm thick, and the proton energy was varied from 250 to 500 keV in 50-keV steps. The experimental $N_{\beta_i}(E)$ curves for the L_{β_1} and L_{β_3} lines excited by protons colliding with antimony atoms are shown in Fig. 3. The error in evaluating N_{β_1} and N_{β_3} does not exceed 5% and is due mainly to inaccuracy in calculating the areas under the peaks; the error in dN_{β_i}/dE amounts to ~15%.

The fluorescence yields ω_1 and ω_2 and the Coster-Kronig factor f_{12} that occur in Eq. (3) were taken from Bambynek's review,^[8] and the total and partial radiative widths Γ_i and Γ_{β_i} , from Scofield's paper.^[9] The x-ray mass absorption coefficients $\bar{\mu}_{\beta_i}$ of the target materials were calculated by Johnson's method.^[10] The values of all these quantities are listed in Table I. The proton stopping powers $S(E)$ of the target materials were determined using the tables of Northcliffe and Schilling.^[11] To estimate the uncertainty in the cross-section ratio due to inaccuracy of the fluorescence yield and the Coster-Kronig factor, the cross-section ratio $\sigma_{L_2}/\sigma_{L_1}$ was calculated for the two values of these quantities available in the literature.^[8] The error in $\sigma_{L_2}/\sigma_{L_1}$ due to inaccuracy of the quantities N_{β_i} and dN_{β_i}/dE is due mainly to the error in the derivative dN_{β_3}/dE and amounts to 20% on the average.

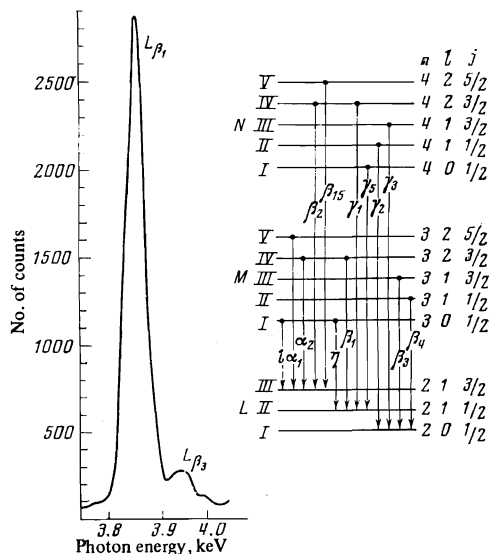


FIG. 2. Part of the x-ray emission spectrum produced by bombarding antimony atoms with 450-keV protons. To the right is a level diagram showing the principal L-series transitions.

2. RESULTS AND DISCUSSION

The experimental results on the ratios of the ionization cross sections for the L_1 and L_2 subshells of palladium, antimony, and lanthanum atoms ($Z=46, 51, 57$) are shown as functions of the incident-proton energy in Fig. 4, where theoretical curves calculated in the Born approximation using the tables of Choi *et al.*^[2] are also shown for comparison. It is evident that the experimental results on the energy dependence of the cross-section ratios $\sigma_{L_2}/\sigma_{L_1}$ agree well with the theoretical results.

It follows from Born-approximation calculations^[1-3] that the ionization cross sections for the L_1 and L_2 subshells of different atoms should depend mainly on the ratio of the proton velocity v to the quantity $(Z_i^*/2)v_0\theta \equiv u_i\sqrt{\theta_i}$, where Z_i^* is the effective nuclear charge for the electron under consideration, $u_i = \sqrt{2I_i/m}$ is a velocity determined from the electron binding energy I_i , and $\theta_i = I_i/(Z_i^*/2)^2 \text{Ry}$ is the outer screening parameter, which is equal to the ratio of the experimental electron binding energy I_i ^[13] to the binding energy $(Z_i^*/2)^2 \text{Ry}$ of an electron in a hydrogenlike system with nuclear charge Z_i^* .

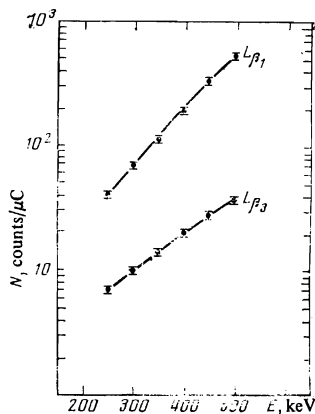


FIG. 3. Intensities of the antimony L_{β_1} and L_{β_3} emission lines vs proton energy E .

TABLE I.

Element	Z	ω_1	ω_2	f_{12}	Γ_1	Γ_{23}	Γ_2	Γ_{31}	$\bar{\mu}_{\beta 1}$, cm ² /g	$\bar{\mu}_{\beta 3}$, cm ² /g
Pd	46	0.0095 ^a 0.0085 ^b	0.052 ^a 0.035 ^b	0.055 ^a 0.060 ^b	0.0380	0.0360	0.1100	0.1000	410	390
Sb	51	0.0200 ^a 0.0311 ^b	0.073 ^a 0.0616 ^b	0.080 ^a 0.164 ^b	0.1188	0.0594	0.1996	0.1715	2E0	260
La	57	0.047 ^a 0.068 ^b	0.098 ^a 0.115 ^b	0.167 ^a 0.190 ^b	0.2190	0.1000	0.348	0.3020	260	250

In this connection, the experimental values of the ionization cross-section ratios for the L_1 and L_2 subshells obtained in the present study using the largest values of the fluorescence yield ratio ω_1/ω_2 and Coster-Kronig factor f_{12} (cases marked "b" in Table I), together with the similar data published up to now^[5-7] for tantalum, gold, lead, and bismuth ($Z = 73, 79, 82,$ and 83) are shown in Fig. 5 as functions of the reduced proton velocity $v/u\sqrt{\theta}$, where $u = (u_{L1} + u_{L2})/2$ and $\theta = (\theta_{L1} + \theta_{L2})/2$. The figure also shows the results of our Born-approximation calculations using Coulomb wave functions for the electron and allowing for outer screening by the method described in Lewis and Merzbacher's review.^[3] The calculations were made for effective charges $Z_{L1} = Z - 3.65$ and $Z_{L2} = Z - 4.65$, in accordance with^[14]. On replacing these values by the Slater values^[15] $Z_{L1}^* = Z_{L2}^* = Z - 4.15$, the calculated values of σ_{L2}/σ_{L1} for atoms with $Z > 50$ increase by no more than 6% while the values of $\theta = (\theta_{L1} + \theta_{L2})/2$ remain virtually unchanged, so that this substitution of effective charges does not change the positions of the experimental points on Fig. 5. Values of σ_{L2}/σ_{L1} calculated for atoms with $Z = 51$ using the tables of Choi *et al.*^[12] are also shown in Fig. 5 for comparison.

It is evident from Fig. 5 that all the experimental values of σ_{L2}/σ_{L1} for atoms with Z from 48 to 83 known up to now lie, in agreement with the results of theoretical calculations, along an average curve giving σ_{L2}/σ_{L1} as a function of $v/u\sqrt{\theta}$. For equal values of $v/u\sqrt{\theta}$ in the range $0.15 \leq v/u\sqrt{\theta} \leq 0.45$, the values of σ_{L2}/σ_{L1} for different atoms differ from one another by no more than a factor of 1.5-2 and agree with the calculated values within about twice the experimental errors. It should be noted that the values of σ_{L2}/σ_{L1} obtained in the present work for atoms with $Z = 46, 51,$ and 57 using the maximum values of ω_1/ω_2 and f_{12} virtually agree with

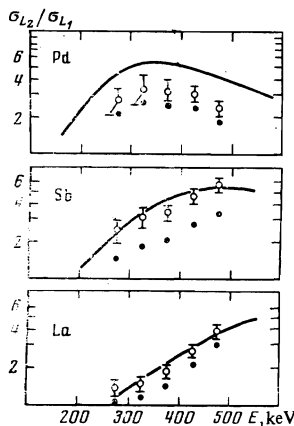


FIG. 4. Experimental ionization cross section ratios for Pd, Sb, and La atoms vs proton energy: the black and open circles represent cross sections obtained using the values of ω_i and f_{12} marked "a" and "b", respectively, in the Table I. The curves were calculated using the tables of Choi *et al.*^[12]

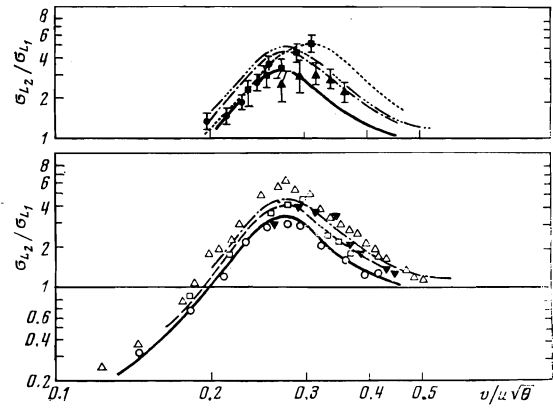


FIG. 5. L_1 - and L_2 -subshell ionization cross section ratio σ_{L2}/σ_{L1} vs reduced proton velocity $v/u\sqrt{\theta}$. The curves represent Born-approximation calculations for the following parameter values: full—for arbitrary Z with $Z_{2s}^* = Z_{2p}^*$ and $\theta = 1$; dashed— $Z = 82$ with $Z_{2s}^* = 78.35$, $Z_{2p}^* = 77.35$, $\theta_{2s} = 0.76$, and $\theta_{2p} = 0.75$; dash-dot— $Z = 51$ with $Z_{2s}^* = 47.35$, $Z_{2p}^* = 46.35$, $\theta_{2s} = 0.62$, and $\theta_{2p} = 0.60$; dash-dot— $Z = 51$ with $Z_{2s}^* = Z_{2p}^* = 46.85$, $\theta_{2s} = 0.63$, and $\theta_{2p} = 0.59$; and dotted— $Z = 51$ with $Z_{2s}^* = Z_{2p}^* = 46.85$, $\theta_{2s} = 0.63$, and $\theta_{2p} = 0.59$, according to the tables of^[12]. The points represent experimental data for Pd (black triangles, base down), Sb (black squares), La (black circles), Ta (black triangles, base up), Au (open triangles), Pb (open squares), and Bi (open circles). The data for Ta, Au, Pb, and Bi, on the lower plot, were taken from^[5-7].

the average values of σ_{L2}/σ_{L1} for atoms with $Z = 73-83$ reported in^[5-7] for the same values of $v/u\sqrt{\theta}$, but if the minimum values of ω_1/ω_2 are used, these cross-section ratios fall about 30% below the average values for the heavy atoms.

It is evident from the experimental data presented in Fig. 5 that in all cases σ_{L2}/σ_{L1} reaches its maximum value of about 3-5 at $v/u\sqrt{\theta} \approx 0.28$. The results of the present study show that the value of σ_{L2}/σ_{L1} near the maximum rises somewhat as Z increases from 46 to 57, whereas according to the results reported in^[5-7], the values of σ_{L2}/σ_{L1} throughout the entire $v/u\sqrt{\theta}$ range from 0.2 to 0.4 decrease by a factor of about 1.5 on the average as Z increases from 79 to 83. In this connection it should be noted that, according to the theoretical calculations, σ_{L2}/σ_{L1} should decrease with increasing nuclear charge Z because of the decrease in the relative difference between the binding energies of L_1 - and L_2 -subshell electrons, and should approach the value, shown on Fig. 5 by the full curve, appropriate for hydrogenlike ions. According to our calculations, the values of σ_{L2}/σ_{L1} in the region $0.2 < v/u\sqrt{\theta} < 0.4$ should decrease by 9-17% as Z increases from 51 to 83.

The experimental data confirm the theoretical conclusion that σ_{L2}/σ_{L1} depends strongly on the incident-proton velocity in the region $v/u\sqrt{\theta} \leq 0.5$. A comparison of the experimental and theoretical results (Fig. 5) shows that the change in the experimental ratio of the cross sections for ionizing the L_1 and L_2 subshells on changing the proton energy is due to the same causes as is the change in σ_{2p}/σ_{2s} in the case of ionization of hydrogenlike particles. But, as was shown in^[11], the change in σ_{2p}/σ_{2s} for

hydrogenlike particles is associated with the fact that when $v/u\sqrt{\theta} \lesssim 0.5$ the ionization cross section is determined by the value of the generalized oscillator strength $f(Q, k)$ in a small range of values of the momentum transfer Q and the momentum k of the ejected electron close to their minimum values $Q_{\min} = I/v$ and $k_{\min} = 0$, and when the proton velocity v decreases, the cross sections change in accordance with the charge in the function $f(Q, k)|_{k=0}$ when Q increases. But the function $f(Q, k)|_{k=0}$ qualitatively reproduces characteristic features of the electron momentum distribution in the initial state, so that in the region of small values of $v/u\sqrt{\theta}$ the ratio σ_i/σ_j of the cross sections for loss of an electron from different states i and j reflects features of the ratio $|\Phi_i(p)|^2/|\Phi_j(p)|^2$ of the electron momentum distributions for these states.¹¹ The maximum in σ_{L2}/σ_{L1} at $v/u\sqrt{\theta} \approx 0.28$ is accordingly due to the node of $2s$ -electron wave function $\Phi_{2s}(p)$ at $p = (Z^*/2)mv_0$, where m is the electron mass, while the decrease in σ_{L2}/σ_{L1} on decreasing and increasing the proton velocity v is due to the decrease in the ratio $|\Phi_{2p}(p)|^2/|\Phi_{2s}(p)|^2$ when p is increased and decreased, respectively.

Thus, the conclusion drawn from the Born-approximation calculations that features of the electrons momentum distribution for the initial state strongly affect the ionization cross section now receives experimental confirmation. However, the experimentally observed increase in σ_{L2}/σ_{L1} on decreasing Z from 83 to 79 and the decrease in this cross-section ratio on decreasing

Z from 57 to 46 apparently require further experimental confirmation and theoretical analysis.

- ¹V. S. Nikolaev, V. S. Senashenko, and V. Yu Shafer, *Phys. Lett.* **31A**, 565 (1970); *J. Phys.* **B6**, 1779 (1973).
- ²V. S. Nikolaev and I. M. Kruglova, *Phys. Lett.* **37A**, 315 (1971).
- ³E. Merzbacher and H. W. Lewis, *Handbuch der Physik*, Vol. **34**, p. 166, Berlin, 1958.
- ⁴J. D. Garcia, R. J. Fortner, and T. M. Kavanagh, *Rev. Mod. Phys.* **45**, 111 (1973).
- ⁵S. Datz, J. L. Guggan, L. C. Feldman, E. Laegsgaard, and J. U. Andersen, *Phys. Rev. A* **9**, 192 (1974).
- ⁶D. H. Madison, A. B. Baskin, C. E. Busch, and S. M. Shafroth, *Phys. Rev. A* **9**, 675 (1974).
- ⁷C. N. Chang, J. F. Morgan, and S. L. Blatt, *Phys. Rev. A* **11**, 607 (1975).
- ⁸Walter Bambynek, Bernd Crasemann, R. W. Fink, H. U. Freund, Hans Mark, C. D. Swift, R. E. Price, and P. Venugopala Rao, *Rev. Mod. Phys.* **44**, 716 (1972).
- ⁹J. H. Scofield, *Phys. Rev.* **179**, 9 (1969).
- ¹⁰M. A. Blokhin, *Fizika rentgenovskikh lucheĭ* (The physics of x rays), Gostekhizdat., 1953.
- ¹¹L. C. Northcliffe and R. E. Schilling, *Nuclear Data Tables*, **A7**, 233 (1970).
- ¹²B. H. Choi, E. Merzbacher, and G. S. Khandelwal, *Atomic Data* **5**, 291 (1973).
- ¹³J. A. Bearden and A. F. Burr, *Rev. Mod. Phys.* **39**, 125 (1967).
- ¹⁴Motoichi Shibuya, *J. Phys. Soc. Japan* **34**, 567 (1973).
- ¹⁵J. C. Slater, *Phys. Rev.* **36**, 57 (1930).

Translated by E. Brunner

Collisional de-excitation of metastable levels and the intensities of the resonance doublet components of hydrogenlike ions in a laser plasma

I. L. Beĭgman, V. A. Boĭko, S. A. Pikuz, and A. Ya. Faenov

P. N. Lebedev Physics Institute, USSR Academy of Sciences
(Submitted March 17, 1976)
Zh. Eksp. Teor. Fiz. **71**, 975-983 (September 1976)

De-excitation of the $2s$ metastable level of hydrogenlike ions by collisions between the ions and charged particles is considered. The measurement of the relative intensities of the fine-structure components of hydrogenlike ions in a laser plasma is described. The experimental data can be explained qualitatively by taking into account de-excitation of the $2s$ level and assuming that the plasma is optically thick relative to the resonance line.

PACS numbers: 52.20.Hv, 52.50.Jm

1. INTRODUCTION

In a plasma, as a rule, the concentration of atoms in metastable states are quite high. Particular interest attaches therefore to the emission lines from these states in collisions with charged particles. The appearance of a charged particle in the vicinity of the atom lifts the "hindrance" on the photon emission and leads to such a sharp increase of the decay probability that the atom has an overwhelming ability of emitting a photon during the collision time. This process is inessen-

tial for levels from which a dipole optical transition is allowed, for in this case the radiative lifetime is much shorter than the characteristic time between the collisions.

The rate of de-excitation of the $2s^1S$ level of the helium atom in collisions with charged particles was calculated in^[1]. A detailed bibliography is given in^[2]. We consider below the de-excitation that occurs during the collision time for an arbitrary multiple interaction, with special attention to the most interesting case of the de-